

FLUORESCENCE QUENCHING DYNAMICS OF TRYPTOPHAN IN PROTEINS

Effect of Internal Rotation under Potential Barrier

FUMIO TANAKA AND NOBORU MATAGA*

*Mie Nursing College, Tsu, Mie 514, Japan; and *Department of Chemistry, Faculty of Engineering Science, Osaka University, Toyonaka, Osaka 560, Japan*

ABSTRACT In many proteins fluorescence from single tryptophan exhibits a nonexponential decay function. To elucidate the origin of this nonexponential decay, we have examined the fluorescence decay function and time-resolved fluorescence anisotropy of a fluorophore covalently bound to a macromolecule by solving a rotational analogue of the Smoluchowski equation. An angular-dependent quenching constant and potential energy for the fluorophore undergoing internal rotation were introduced into the equation of motion for fluorophore. Results of numerical calculations using the equations thus obtained predict that both the fluorescence decay function and time-resolved anisotropy are dependent on rotational diffusion coefficients of fluorophore and potential energy for the internal rotation. The method was applied to the observed fluorescence decay curve of the single tryptophan in apocytochrome *c* from horse heart. The calculated decay curves fit the observed ones well.

INTRODUCTION

Recent experimental (Gurd and Rothgeb, 1979) and theoretical (Karplus and McCammon, 1983) works have revealed that protein structure is inherently dynamic. Beechem and Brand (1985) have reviewed recent works demonstrating that aromatic amino acid residues such as tryptophan (Trp) and tyrosine (Tyr) possess a motional freedom of internal rotation during their fluorescence lifetime, even if they are buried in protein matrices. With respect to this problem, we have demonstrated previously (Tanaka and Mataga, 1982) that the fluorescence decay function of an energy donor in proteins should be nonexponential when the transfer is faster than the internal rotation. The nonexponential nature of the decay curve of single tryptophan was observed in myoglobin from tuna, where fluorescence from Trp-14 was strongly quenched due to efficient energy transfer to heme (Hochstrasser and Negus, 1984). However, apomyoglobin from tuna (Hochstrasser and Negus, 1984) and many other proteins with single tryptophan (Beechem and Brand, 1985) exhibited nonexponential decay, even though the acceptor is absent in the proteins.

To elucidate the underlying mechanism of these phenomena, we have developed a model that takes into consideration the effect of internal rotation of a fluorophore covalently bound to a protein on the fluorescence decay function and time-resolved fluorescence anisotropy

based on a more general theoretical treatment than the previous one (Tanaka and Mataga, 1982). In the present model, we introduced an angular-dependent fluorescence quenching constant into a rotational analogue of the Smoluchowski equation (Favro, 1958, 1960), which has been frequently used for the studies of electron spin resonance (ESR) line shape (Nordio et al., 1972; Polnaszek et al., 1973; Polnaszek and Freed, 1975), nuclear spin relaxation (Bernassau et al., 1982), and fluorescence depolarization (Kinoshita et al., 1977; Burghardt, 1985). Burghardt (1983, 1984, 1985) has demonstrated that the method of spherical tensor (Landau and Lifshitz, 1983; Rose, 1971) is useful for solving a rotational diffusion equation of a rigid rotor, and has applied it to the problems of time-resolved fluorescence anisotropy. In the present work, we have extended the method to a model that includes an angular-dependent quenching constant as stated above and have applied it to the analysis of fluorescence decay curves of tryptophan in proteins.

EXPERIMENTAL PROCEDURE

Cytochrome *c* from horse heart (Type VI) was purchased from Sigma Chemical Co. (St. Louis, MO). It was purified by column chromatography on CM cellulose (CM-32; Nakarai Chemicals, Ltd., Kyoto, Japan) with 85 mM phosphate buffer at pH 7.0, and then on hydroxyapatite (DNA grade; Bio-Rad Laboratories, Richmond, CA) under an ionic strength gradient between 20 and 500 mM of phosphate. Apocytochrome *c* was prepared by removing heme from the purified cytochrome *c* according to the method reported by Sano and Tanaka (1964).

Fluorescence decay curves of tryptophan of apocytochrome *c* were measured with a time-correlated single-photon counting method using a

Address offprint requests to Dr. Noboru Mataga.

synchronously pumped, cavity-dumped dye laser for excitation (at 295 nm). Details of the experimental arrangement are described elsewhere (Yamazaki et al., 1985).

THEORETICAL MODEL

We model the tryptophan residue as a completely asymmetric rotor covalently bound to a spherical protein. Geometrical arrangement of the molecular systems and experimental laboratory system is illustrated in Fig. 1. The fluorophore possesses motional freedom of internal rotation about covalent bonds in the macromolecule. The internal rotation was described with Euler angles of $\omega = (\alpha\beta\gamma)$ from the macromolecular system (x', y', z') to the tryptophan system (x, y, z). The experimental laboratory system was shown with (X, Y, Z) coordinate axes. Transformation of the motion of spherical protein from the (X, Y, Z) system to the (x', y', z') system was described with Euler angles of $\Omega = (\psi\theta\phi)$. Transition moments of absorption and emission of tryptophan are shown by \mathbf{m}_a and \mathbf{m}_e in the (x, y, z) system, respectively. Directions of \mathbf{m}_a and \mathbf{m}_e are represented with polar coordinate angles as $\omega_a = (\epsilon_a\delta_a)$ and $\omega_e = (\epsilon_e\delta_e)$ in (x, y, z).

Green's function, $G(\Omega'\omega\Omega\omega't)$, for the rotational motion of fluorophore was described by a diffusion equation for the spherical protein and by the rotational analogue of the

Smoluchowski equation (Favro, 1958) for the internal motion of the fluorophore.

$$\begin{aligned} \frac{\partial}{\partial t} G(\Omega'\omega\Omega\omega't) = & -[k_1 + k_q(\omega)] G(\Omega'\omega\Omega\omega't) \\ & - (D\mathbf{J}_\Omega^2 + \mathbf{J}_\omega \cdot \mathbf{D}_I \cdot \mathbf{J}_\omega) G(\Omega'\omega\Omega\omega't) \\ & - \frac{1}{2kT} \mathbf{J}_\omega \cdot \mathbf{D}_I \cdot \mathbf{J}_\omega V(\omega) G(\Omega'\omega\Omega\omega't) \\ & + \frac{1}{(2kT)^2} [\mathbf{J}_\omega V(\omega)] \cdot \mathbf{D}_I \cdot [\mathbf{J}_\omega V(\omega)] G(\Omega'\omega\Omega\omega't), \end{aligned} \quad (1)$$

where k_1 is the decay constant of excitation of fluorophore without quencher, D is the rotational diffusion coefficient of spherical protein, and \mathbf{D}_I is the second rank tensor of the rotational diffusion coefficient of internal motion of fluorophore. k is the Boltzmann constant and T , temperature. Angular momentum operators for the spherical rotor and the completely asymmetric rotor are represented by \mathbf{J}_Ω and \mathbf{J}_ω , respectively. The fluorescence quenching constant and potential energy were expanded with a generalized spherical harmonic as Eqs. 2 and 3, respectively.

$$k_q(\omega) = \sum_{l=0}^{\infty} \sum_{m=-l}^l \sum_{m'=-l}^l A_{mm'}^l D_{mm'}^{(l)}(\omega) \quad (2)$$

$$V(\omega) = \sum_{l=0}^{\infty} \sum_{m=-l}^l \sum_{m'=-l}^l B_{mm'}^l D_{mm'}^{(l)}(\omega), \quad (3)$$

where $A_{mm'}^l$ and $B_{mm'}^l$ are constants, and $D_{mm'}^{(l)}(\omega)$ is the generalized spherical harmonic (Landau and Lifshitz, 1983). To insure that $k_q(\omega)$ and $V(\omega)$ are real functions, the relations, $A_{mm'}^l = (-1)^{m+m'} A_{-m-m'}^l$ and $B_{mm'}^l = (-1)^{m+m'} B_{-m-m'}^l$ should be held.

Eq. 1 may be solved by using Green's function in the form of Eq. 4.

$$G(\Omega'\omega\Omega\omega't) = \sum_{n=0}^{\infty} \sum_{m=-n}^n Y_{nm}^*(\Omega') Y_{nm}(\Omega) \cdot \sum_{\kappa=1}^{\infty} \psi_{\kappa}^*(\omega) \psi_{\kappa}(\omega') e^{\lambda_{\kappa} t}, \quad (4)$$

where $Y_{nm}(\Omega)$ is a spherical harmonic and eigen function for the spherical rotor, and $\psi_{\kappa}(\omega)$ is an eigen function for the asymmetric rotor and expanded in terms of eigen functions for the symmetric rotor as indicated in Eq. 5

$$\psi_{\kappa}(\omega) = \sum_{p=0}^{\infty} \sum_{q,q'=-p}^p C_{qq'}^{\kappa p} \Phi_{qq'}^p(\omega), \quad (5)$$

where $\Phi_{qq'}^p(\omega)$ is an eigen function for the symmetric rotor (Landau and Lifshitz, 1983) as shown in Eq. 6

$$\Phi_{qq'}^p(\omega) = (i)^p \left(\frac{2p+1}{8\pi^2} \right)^{1/2} D_{q'q}^{(p)}(\omega). \quad (6)$$

Expansion coefficients, $C_{qq'}^{\kappa p}$ ($\kappa = 1, 2, 3, \dots; p = 0, 1, 2, \dots; q, q' = -p$ to p), are obtained as eigen vectors

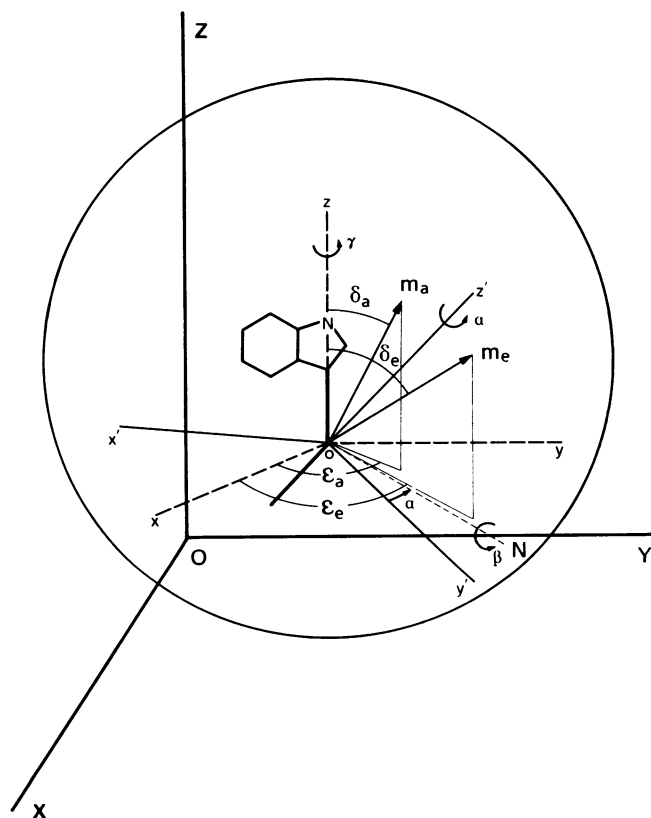


FIGURE 1 Geometrical arrangement of molecular and experimental laboratory systems. Details are described in text.

corresponding to eigen values, λ_{nk} , of a set of simultaneous linear equations derived from Eq. 1 (see Appendix).

FLUORESCENCE DECAY FUNCTION AND TIME-RESOLVED ANISOTROPY

Transition moments of absorption, \mathbf{m}_a , and emission, \mathbf{m}_e , represented in the (x, y, z) system were expressed as \mathbf{M}_a and \mathbf{M}_e , respectively, in the experimental laboratory system with a transformation matrix with rotational angles of ω from the (x, y, z) system to the (x', y', z') system and with rotational angles of Ω from the (x', y', z') system to the (X, Y, Z) system. Measurements of time-resolved fluorescence anisotropy are made by exciting the sample placed at O with a polarized light beam along the Z-axis in the direction of the X-axis. Polarized fluorescence along the Z-axis or X-axis is observed in the direction of the Y-axis (Tanaka and Mataga, 1982).

The excitation probability of fluorophore upon excitation with polarized light along the Z-axis may be obtained by Eq. 7 (Chuang and Eisenthal, 1972; Tanaka and Mataga, 1982).

$$\rho(\Omega\omega t) = \int d\Omega' \int d\omega' M_{aZ}^2 \exp \left[\frac{V(\omega') - V(\omega)}{2kT} \right] G(\Omega'\omega\Omega\omega't). \quad (7)$$

M_{aZ}^2 can be expressed with generalized spherical harmonics (Landau and Lifshitz, 1983; Rose, 1971). The Boltzmann factor may be expanded also in terms of generalized spherical harmonics after substituting Eq. 3 for potential energy.

Fluorescence intensity and time-resolved anisotropy can be obtained from the excitation probability and transition moments of emission (Chuang and Eisenthal, 1972; Tanaka and Mataga, 1982). The transition moments may be also expressed with generalized spherical harmonics (Landau and Lifshitz, 1983; Rose, 1971). The fluorescence decay function can be obtained as Eq. 8.

$$\begin{aligned} F(t) &= \int d\Omega \int d\omega \{M_{eZ}^2 + 2M_{eX}^2\} \rho(\Omega\omega t) \\ &= \frac{1}{3} \sum_{\kappa=1}^{\infty} e^{\lambda_{0\kappa} t} [|C_{00}^{\kappa 0}|^2 \\ &\quad + \frac{1}{(2kT)^2} \sum_{l=0}^{\infty} \sum_{mm'=-l}^l \frac{1}{2l+1} |B_{mm'}^l|^2 |C_{00}^{\kappa 0}|^2 \\ &\quad - |C_{-m,-m'}^l|^2] \\ &\quad + \frac{1}{2} \frac{1}{(2kT)^3} \sum_{l=0}^{\infty} \sum_{mm'=-l}^l \sum_{u=0}^{\infty} \\ &\quad \cdot \sum_{L=|l-u|}^{l+u} \sum_{MM'=-L}^L \frac{(-1)^{M+M'}}{2L+1} \\ &\quad \cdot C(luL; m, -M-m) C(luL; m', -M'-m') \\ &\quad \cdot B_{mm'}^l B_{-M-m,-M'-m'}^u B_{MM'}^L \end{aligned}$$

$$\begin{aligned} &\cdot [|C_{-M,-M'}^L|^2 - |C_{MM'}^L|^2] \\ &+ \frac{1}{4} \frac{1}{(2kT)^4} \left\{ \frac{1}{3} \sum_{l=0}^{\infty} \sum_{mm'=-l}^l \sum_{u=0}^{\infty} \right. \\ &\cdot \sum_{p=0}^{\infty} \sum_{qq'=-p}^p \sum_{g=0}^{\infty} \sum_{L=|l-u|}^{l+u} \sum_{MM'=-L}^L \\ &\cdot \frac{(-1)^{M+M'}}{2L+1} C(luL; m, M-m) C(luL; m', M'-m') \\ &\cdot C(pgL; q, -M-q) C(pgL; q', -M'-q') \\ &\cdot B_{mm'}^l B_{-M-m,-M'-m'}^u B_{qq'}^p B_{-M-q,-M'-q'}^g |C_{00}^{\kappa 0}|^2 \\ &- \frac{2}{3} \sum_{l=0}^{\infty} \sum_{mm'=-l}^l \sum_{u=0}^{\infty} \sum_{p=0}^{\infty} \\ &\cdot \sum_{qq'=-p}^p \sum_{g=0}^{\infty} \sum_{L=|l-u|}^{l+u} \sum_{MM'=-L}^L \frac{(-1)^{M+M'}}{2L+1} \\ &\cdot C(luL; m, M-m) C(luL; m', M'-m') \\ &\cdot C(pgL; q, -M-q) C(pgL; q', -M'-q') \\ &\cdot B_{mm'}^l B_{-M-m,-M'-m'}^u B_{qq'}^p B_{-M-q,-M'-q'}^g \\ &\cdot [|C_{M+q,M'+q'}^{\kappa g}|^2 + |C_{-M-q,-M'-q'}^{\kappa g}|^2] \\ &+ \sum_{l=0}^{\infty} \sum_{mm'=-l}^l \sum_{u=0}^{\infty} \sum_{p=0}^{\infty} \\ &\cdot \sum_{qq'=-p}^p \sum_{g=0}^{\infty} \sum_{L=|l-p|}^{l+p} \sum_{MM'=-L}^L \frac{(-1)^{M+M'}}{2L+1} \\ &\cdot C(luL; m, M-m) C(luL; m', M'-m') \\ &\cdot C(pgL; q, -M-q) C(pgL; q', -M'-q') \\ &\cdot B_{mm'}^l B_{-M-m,-M'-m'}^u B_{qq'}^p B_{-M-q,-M'-q'}^g \\ &\cdot |C_{-M,-M'}^L|^2 \Big\} \\ &+ \dots \dots \dots \Big]. \quad (8) \end{aligned}$$

Expressions for time-resolved fluorescence anisotropy can be written as

$$\begin{aligned} A(t) &= \frac{1}{F(t)} \int d\Omega \int d\omega (M_{eZ}^2 - M_{eX}^2) \rho(\Omega\omega t) \\ &= \frac{2}{75} \frac{1}{F(t)} \sum_{\kappa=0}^{\infty} e^{\lambda_{2\kappa} t} \sum_{qq'=-2}^2 \\ &\cdot \left\{ D_{0,-q}^{(2)}(\omega_a) D_{0,-q}^{*(2)}(\omega_e) |C_{qq'}^{\kappa 2}|^2 \right. \\ &+ \frac{1}{2kT} \sum_{l=0}^{\infty} \sum_{m=-l}^l (-1)^m C(2l2; qm) C(2l2; q'0) B_{m0}^l \\ &\cdot D_{0,-q-m}^{(2)}(\omega_a) D_{0,-q}^{*(2)}(\omega_e) [|C_{qq'}^{\kappa 2}|^2 - |C_{q+m,q'}^{\kappa 2}|^2] \\ &+ \frac{1}{(2kT)^2} \frac{1}{2} \sum_{l=0}^{\infty} \sum_{mm'=-l}^l \sum_{u=0}^{\infty} \sum_{L=|l-u|}^{l+u} \\ &\cdot \sum_{M=-L}^L (-1)^M B_{mm'}^l B_{-M-m,-m'}^u \end{aligned}$$

$$\begin{aligned}
& \cdot C(luL; m, M - m) C(luL; m', -m') \\
& \cdot C(2L2; qM) C(2L2; q'0) \\
& \cdot D_{0,-q-M}^{(2)}(\omega_a) D_{0,-q}^{*(2)}(\omega_e) \\
& \cdot \{ |C_{qq'}^{\kappa 2}|^2 + |C_{q+M,q'}^{\kappa 2}|^2 \} \\
& - \frac{1}{(2kT)^2} \sum_{l=0}^{\infty} \sum_{mm'=-l}^l \sum_{u=0}^{\infty} \sum_{v=-u}^u \\
& \cdot \sum_{L=|l-2|}^{l+2} B_{mm'}^l B_{v,-m'}^u \\
& \cdot C(2lL; -q - m - v, m) C(2lL; -q', m') \\
& \cdot C(Lu2; -q - v, v) C(Lu2; -q' + m', -m') \\
& \cdot D_{0,-q-m-v}^{(2)}(\omega_a) D_{0,-q}^{*(2)}(\omega_e) \\
& \cdot |C_{q+v,q'-m'}^{\kappa L}|^2 \\
& + \dots \dots \dots \} \quad (9)
\end{aligned}$$

NUMERICAL CALCULATIONS FOR MODEL CASES

We have calculated the fluorescence decay function and time-resolved anisotropy for model cases. The dependence of fluorescence decay function upon rotational diffusion coefficients is shown in Fig. 2. The potential energy for internal rotation of fluorophore was neglected in this

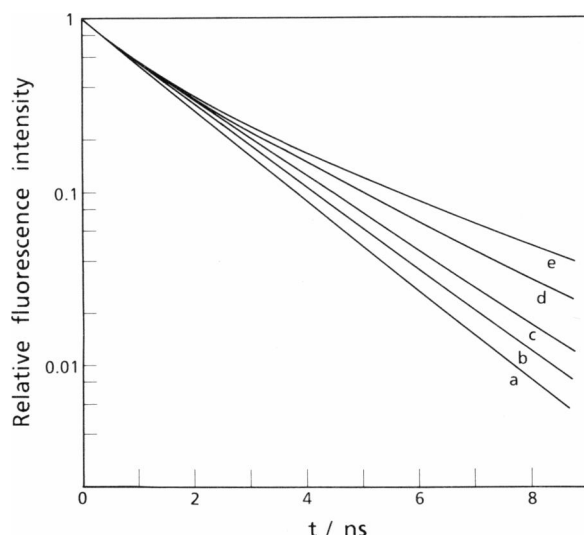


FIGURE 2 Dependence of fluorescence decay function upon rotational diffusion coefficients. Decay functions were calculated for various rotational diffusion coefficients. Potential energy was neglected in the calculations. k_1 was taken to be 0.1 ns^{-1} . $k_q(\alpha\beta)$ was approximated by Eq. 10. Diffusion coefficients were expressed by a tensor of second rank, whose components were D_{xx} , D_{yy} , D_{zz} , D_{xy} , D_{yz} , and D_{zx} . The values of the components for the decay functions *a* to *e* are given in this order as follows: *a*, ∞ , ∞ , 0.15 , 0.15 , 0.15 ; *b*, 1.0 , 1.0 , 1.0 , 0.15 , 0.15 , 0.15 ; *c*, 0.5 , 0.5 , 0.5 , 0.15 , 0.15 , 0.15 ; *d*, 0.2 , 0.2 , 0.2 , 0.15 , 0.15 , 0.15 ; *e*, 0.1 , 0.1 , 0.1 , 0.15 , 0.15 , 0.15 ns^{-1} .

calculation. The value of k_1 was 0.1 ns^{-1} . The quenching constant was approximated by Eq. 10.

$$k_q(\alpha\beta) = 0.5 + \frac{1}{2} \sin\alpha \sin\beta - \frac{1}{4} \cos\beta \text{ (ns}^{-1}\text{)}, \quad (10)$$

where $k_q(\alpha\beta)$ is expressed in terms of spherical harmonics, $Y_{1m}(\alpha\beta)$ ($m = -1, 0, 1$). Eq. 10 is just the first and second terms in the expansion with spherical harmonics in Eq. 2. In order to describe $k_q(\omega)$ of real systems exactly we may need the expansion of Eq. 2 to higher orders, which makes the actual analyses difficult. Diffusion coefficients form a second rank tensor. In Fig. 2 we assumed that diagonal coefficients are all equal and nondiagonal coefficients are also all equal to each other. As we can see from Fig. 2, decay function is single exponential when the diagonal coefficients are large enough. However, it becomes nonexponential as internal rotation becomes slower. Fig. 3 shows dependence of time-resolved anisotropy upon diffusion coefficients of internal rotation. The diffusion coefficient of the macromolecule was taken to be 0.01 ns^{-1} . Directions of \mathbf{m}_a and \mathbf{m}_e were both taken along *z*-axis. The other conditions were the same as in Fig. 2. Fig. 3 shows clearly that time-resolved anisotropy is strongly dependent upon the diffusion coefficients of internal motion.

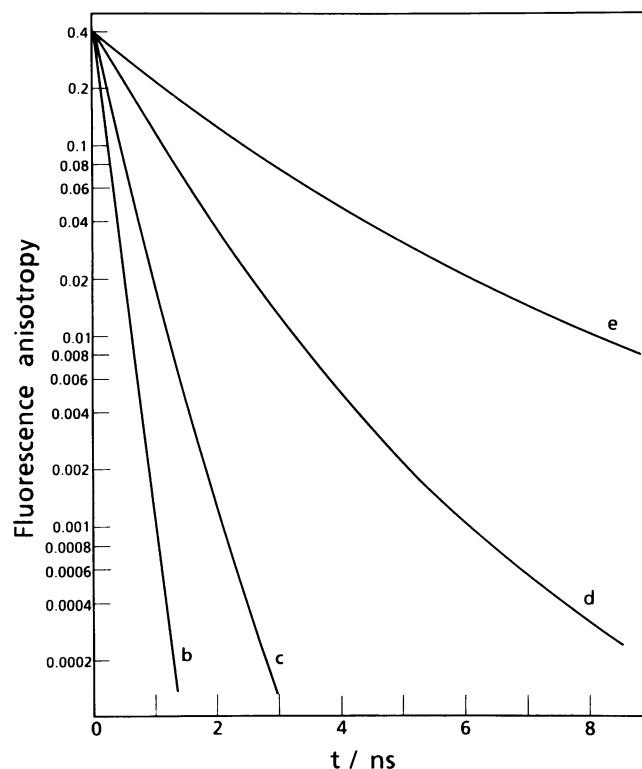


FIGURE 3 Dependence of time-resolved anisotropy upon rotational diffusion coefficients. Fluorescence anisotropy decay was calculated varying rotational diffusion coefficients. Potential energy was neglected. Diffusion coefficient of macromolecule was taken to be 0.01 ns^{-1} . Directions of \mathbf{m}_a and \mathbf{m}_e were both along the *z*-axis. The other parameters were same as those in Fig. 2.

The dependence of fluorescence decay function upon potential energy was also examined. The quenching constant was assumed to be the same as in Eq. 10. Potential energy was expressed by Eq. 11. Fluorescence decay profiles at different potentials are shown by curves *a*, *b*, *c*, and *d* in Fig 4.

$$V(\alpha\beta) = 1.0 - p(\sin\alpha\sin\beta - \frac{1}{2}\cos\beta) \quad (\text{in units of } kT). \quad (11)$$

The height of potential energy was varied by changing the value of *p*. The value of k_1 was taken to be 0.1 ns^{-1} . As we can see from Fig. 4 the fluorescence decay function is also dependent on the height of potential energy. The nonexponential nature of the decay function is reduced as the height of potential energy is increased. However, when the dependence of potential energy on rotational angles of internal motion shown in Eq. 12 is similar to that of the quenching constant expressed in Eq. 10, nonexponential nature becomes enhanced, as demonstrated in curve *e* of Fig. 4.

$$V(\alpha\beta) = 1.0 + \sin\alpha\sin\beta - \frac{1}{2}\cos\beta \quad (\text{in units of } kT). \quad (12)$$

Namely, at rotational angles where the quenching constant exhibits the maximum, potential energy is also highest. Accordingly, the population of fluorophore at angles with the maximum quenching constant should be very small. Therefore, it is reasonable to expect to see a slowly decaying decay function as shown by curve *e* in Fig. 4.

The dependence of time-resolved anisotropy upon potential energy was also examined and shown in Fig. 5. The diffusion coefficient of the macromolecule was 0.01 ns^{-1} . The directions of \mathbf{m}_s and \mathbf{m}_e were both along the *z*-axis. The other parameters for the calculations were the same as

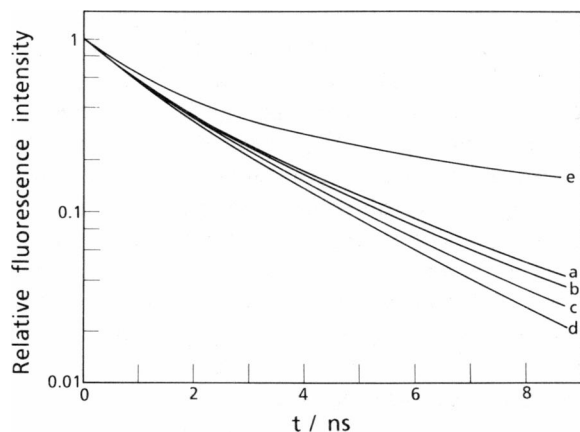


FIGURE 4 Dependence of fluorescence decay function upon potential energy. Fluorescence decay function was calculated with varying height of potential energy. k_1 was taken to be 0.1 ns^{-1} . $k_q(\alpha\beta)$ was approximated by Eq. 10. Dependence of potential energy on rotational angles of internal motion in *a*–*d* was expressed by Eq. 11. The values of *p* were 0.0 in *a*; 0.2 in *b*; 0.6 in *c*; 1.0 in *d*. Dependence of potential energy on rotational angles of internal motion in *e* was represented by Eq. 12. The values of diffusion coefficients were the same as those of *e* in Figs. 2 and 3.

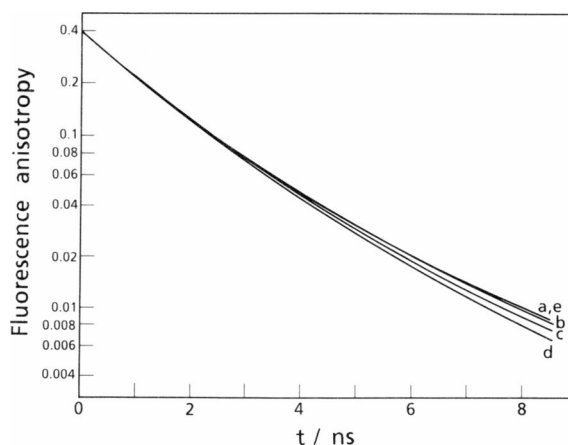


FIGURE 5 Dependence of time-resolved anisotropy upon potential energy. Diffusion coefficient of spherical macromolecule was taken to be 0.01 ns^{-1} . Directions of \mathbf{m}_s and \mathbf{m}_e were both along the *z*-axis. The other parameters for the calculations were the same as those in Fig. 4.

those in Fig. 4. The dependence of time-resolved anisotropy upon height of potential energy was little, even if the shape of potential energy was changed.

FLUORESCENCE DECAY ANALYSIS OF APOCYTOCHROME *c* FROM HORSE HEART

Cytochrome *c* from horse heart possesses single tryptophan (Trp 59) residue. The three-dimensional structure of cytochrome *c* from horse heart has been determined at the resolution of 2.8 \AA (Dickerson et al., 1975). Fluorescence from Trp-59 is strongly quenched due to the energy transfer to heme located within 10 \AA of Trp-59. One of the propionic acids of the heme is hydrogen-bonded to N-H of Trp-59 and the other is hydrogen-bonded to OH of Tyr-48. After heme is removed, Trp-59 could have appreciable freedom of internal rotation. Fluorescence decay curves of Trp-59 measured at 35° and 5°C exhibited nonexponential decay. Observed decay curve obtained at 35°C is shown in Fig. 6 and at 5°C in Fig. 7. We have analyzed these decay curves by the present method using Eq. 8. We assumed that the OH group of Tyr-48 is an effective quencher for Trp-59 and $k_q(\chi)$ is given by Eq. 13.

$$k_q(\chi) = a(1 + \cos\chi), \quad (13)$$

where χ is a solid angle between a vector formed by the center of the indole ring of Trp-59 and the origin, and a vector formed by the O atom of Tyr-48 and the origin (see Fig. 1). $\cos\chi$ is given by a first-order Legendre polynomial, which is again expanded by the first-order spherical harmonics with variables of α and β as represented by Eq. 14.

$$\cos\chi = (4\pi/3) \sum_{m=-1}^1 Y_{1m}^*(\alpha_q\beta_q) Y_{1m}(\alpha\beta), \quad (14)$$

where α_q and β_q denote angular part of polar coordinates of quencher. We have used 0.1163 ns^{-1} as the k_1 value, which

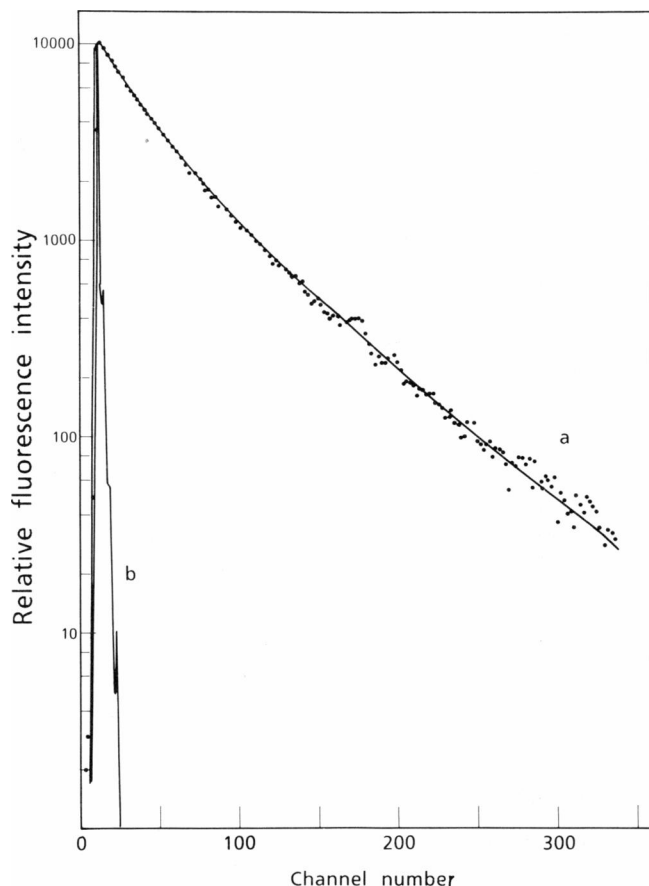


FIGURE 6 Fluorescence decay curve of tryptophan residue of apocytochrome *c* at 35°C. Cytochrome *c* contains single tryptophan (Trp-59) residue. Fluorescence of Trp-59 was strongly quenched due to energy transfer to heme. When heme was removed Trp-59 became fluorescent. The fluorescence decay curve of Trp-59 in apocytochrome *c* was nonexponential and simulated with decay function of the present model. The calculated decay curve is shown with a solid curve in *a*. Excitation pulse is shown by *b*. The time interval per channel was 51.2 ps. Parameters used for the calculation are as follows: $k_1 = 0.1163 \text{ ns}^{-1}$ and $k_q(\chi) = 0.535 (1 + \cos \chi) \text{ ns}^{-1}$. The explicit form of $\cos \chi$ is represented by Eq. 14. We assumed that the OH of tyrosine 48 (Tyr-48) existing near by Trp-59 is an effective quencher. χ represents an angle between the vector formed by center of Trp-59 and the origin in the (x', y', z') system, and the vector formed by an oxygen atom of OH and origin in the (x', y', z') system. Rotational diffusion coefficients were $D_{xx} = D_{yy} = D_{zz} = 0.04$ and $D_{xy} = D_{yz} = D_{zx} = 0.0005$ in ns^{-1} . Potential energy was negligibly small.

is the inverse of the longest lifetime of free tryptophan obtained in alkaline solution (Jameson and Weber, 1981). We also assumed that all values of diagonal diffusion coefficients are equal (D_d), and further, all values of nondiagonal diffusion coefficients are equal (D_n). First, we neglected potential energy. Geometrical factors were calculated from three-dimensional structure of oxydized cytochrome *c* from tuna (Takano and Dickerson, 1981). The calculated decay curve was obtained from Eq. 15.

$$I_c(t) = \int_0^t dt' E(t') F(t - t'), \quad (15)$$

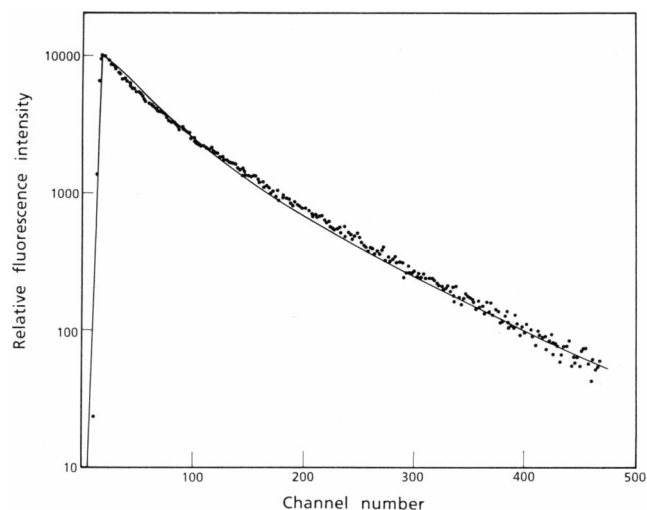


FIGURE 7 Fluorescence decay curve of tryptophan residue of apocytochrome *c* at 5°C. Calculated decay curve is shown with a solid curve. The time interval per channel was 51.2 ps. Parameters used for the calculation are as follows: $k_1 = 0.1163 \text{ ns}^{-1}$, $k_q(\chi) = 0.33 (1 + \cos \chi) \text{ ns}^{-1}$, $V(\chi) = 1.5 (1 + \cos \chi)$ (in kT units), $D_{xx} = D_{yy} = D_{zz} = 0.0005 \text{ ns}^{-1}$, and $D_{xy} = D_{yz} = D_{zx} = 0.00005 \text{ ns}^{-1}$.

where $E(t)$ is an excitation pulse and $F(t)$ is the decay function obtained from Eq. 8 after various assumptions stated above. The values of a , D_d , and D_n were systematically varied so as to obtain the minimum value of χ^2 given by Eq. 16.

$$\chi^2 = \sum_{i=1}^n \frac{1}{n} \frac{[I_o(t_i) - I_c(t_i)]^2}{I_o(t_i)}, \quad (16)$$

where $I_o(t_i)$ is the observed decay curve of Trp-59 in apocytochrome *c*.

The best fitting of the observed decay curve at 35°C to the calculated one was obtained with the values of $a = 0.535 \text{ ns}^{-1}$, $D_d = 0.040 \text{ ns}^{-1}$, and $D_n = 0.0005 \text{ ns}^{-1}$. The calculated decay curve with these values is indicated by the solid curve in Fig. 6. Improvement of fitting between observed and calculated decay curves was not obtained by employing a few different types of potential energy expressed by using $Y_{1m}(\alpha\beta)$. The fitting procedure was also applied to the decay curve obtained at 5°C. In this case, however, the fitting was rather poor, even if different types of potential energy expressed with $Y_{1m}(\alpha\beta)$ ($m = -1, 0, 1$) were introduced into Eq. 8. The best fit was obtained when potential energy was expressed by Eq. 17.

$$V(\chi) = b (1 + \cos \chi). \quad (17)$$

This means that potential energy is maximum in the direction of quencher. In this case, parameters at the best fitting were $a = 0.33 \text{ ns}^{-1}$, $b = 1.5$ (in units of kT), $D_d = 0.0005 \text{ ns}^{-1}$, and $D_n = 0.00005 \text{ ns}^{-1}$. The calculated decay curve with these parameters was represented by the solid curve in Fig. 7. It is noted that the diffusion coefficients

were smaller at 5°C than at 35°C and potential energy was higher at the lower temperature than at the higher temperature. The values of a , which represents an averaged value of $k_q(\chi)$ over α and β , depended on temperature. At the present stage of investigation, however, it is difficult to derive any quantitative conclusion concerning the results at 5°C since the approximations used for the calculation of the decay function are rather crude.

DISCUSSION AND CONCLUDING REMARKS

We have obtained the expressions for fluorescence decay function and time-resolved fluorescence anisotropy of a completely asymmetric fluorophore covalently bound to a spherical macromolecule in the presence of an angular-dependent quenching process and potential energy for the fluorophore undergoing internal rotation. Results of numerical calculations for some model systems using the equations thus obtained predict that both the fluorescence decay function and time-resolved fluorescence anisotropy are strongly dependent on rotational diffusion coefficients of fluorophore. When the internal rotation is fast compared with an averaged decay constant of fluorophore over the rotational angles, the decay function was predicted to be single exponential. However, as the internal rotation becomes slower, the decay function should exhibit nonexponential behavior. Moreover, whenever time-resolved anisotropy is observable during the fluorescence lifetime, the decay function should always be nonexponential. The effects of the presence of potential energy for the internal rotation were more significant on the decay function than on the time-resolved anisotropy. However, it is not clear at the present stage of investigation whether the time-resolved anisotropy is dependent not so much on the potential energy but rather on the diffusion coefficients since our model calculations were made for rather extreme cases.

We have applied the present method to the observed fluorescence decay curve of single tryptophan in apocytocrome *c*. Both the decay curves obtained at 35° and 5°C exhibited nonexponential decay. Agreement between observed and calculated decay curves was excellent for the one obtained at the higher temperature without introducing potential energy. Diffusion coefficients of internal rotation were 0.040 ns⁻¹ for diagonal ones and 0.0005 ns⁻¹ for nondiagonal ones. All coefficients were much smaller than the averaged decay constant of Trp-59 (0.65 ns⁻¹). In the present results the values of a depended on temperature. The temperature-dependence of a may be explained as follows: Trp could have many other motional freedoms including vibrations besides the rotations over α and β . If the other motions were fast compared with the fluorescence emission, then the value of $k_q(\chi)$ could be averaged over those nuclear motions according to equilibrium thermodynamics. Hence, a should depend on temperature.

We have expressed the fluorescence quenching constant only as a function of rotational variables of internal motion, although usually it strongly depends on the distance between Trp and a quencher. Our approximation may be reasonable since the distance could not change much in proteins. The quenching constant should always be dependent on the mutual orientation between Trp and the quencher whatever the mechanism of the quenching is, although the orientational dependence of a quenching constant was not taken into account explicitly so far, except for the case of excitation energy transfer (Tanaka and Mataga, 1982).

A number of works have reported on the fluorescence lifetime of single tryptophan in proteins (Beechem and Brand, 1985). In nuclease *B* and melittin, fluorescence decay curves of single tryptophan were confirmed to be mono-exponential. No internal rotation of tryptophan residues in these proteins was observed by time-resolved anisotropy measurements. In many other proteins containing single tryptophan, however, it is suggested that tryptophan residues, whose internal rotations are not very fast, show nonexponential fluorescence decay. These observations support our model that connects the internal motion of tryptophan residue in proteins with its fluorescence decay function and time-resolved fluorescence anisotropy.

Recently, a potential energy was introduced into the expression for time-resolved anisotropy by Burghardt (1985) using the Smoluchowski equation given by Favro (1958). Differences between our model and the one proposed by Burghardt are as follows: (a) potential energy was introduced for the internal motion of the asymmetric fluorophore and the motion of the spherical macromolecule was assumed to be free in the present work, while the introduction of a potential energy was performed for the motion of asymmetric macromolecule, and internal motion of fluorophore was neglected in the work by Burghardt (1985); (b) the angular dependence of the quenching constant was taken into account in the present work while it was not considered in the work by Burghardt, and (c) we have chosen the direction of the covalent bond between CH₂ and the indole ring as the *z*-axis while Burghardt chose the direction along one of the principal axes of fluorophore as the *z*-axis. Introduction of off-diagonal diffusion coefficients due to our choice of *z*-axis is a most general treatment and could enable us to make various analyses on the rotational mode of a fluorophore covalently bound to protein. When the off-diagonal diffusion coefficients are put equal to zero, our treatment reduces to the case where the orientation of the tryptophan coordinate system is chosen as the principal axis frame. With the assumption that the fluorescence quenching constant does not depend on the internal rotation, it may be difficult to explain the nonexponential decay profile of tryptophan in proteins (Beechem and Brand, 1985). It should be noted that time-resolved anisotropy can be affected by the

quenching constant and conversely fluorescence decay function can also be modified not only by the diffusion coefficients but also by the presence of potential energy for the motion of fluorophore when the decay function is not single exponential.

APPENDIX

Expansion coefficients, C_{qq}^p , and decay constants, λ_m , were obtained by the method of spherical tensor for internal motion (Landau and Lifshitz, 1983; Rose, 1971; Burghardt, 1983). The following simultaneous linear equations were derived from Eq. 1 in the text.

$$\begin{aligned}
 & - \left[\lambda_n + k_1 + n(n+1)D + \frac{1}{(3)^{1/2}} r(r+1)R_{00} \right] C_{ss}^r \\
 & + \frac{1}{(20)^{1/2}} \\
 & \cdot R_{2,-2} [(r+s+1)(r-s)(r+s+2)(r-s-1)]^{1/2} C_{s+2,s}^r \\
 & + \frac{2s+1}{(20)^{1/2}} R_{2,-1} [(r-s)(r+s+1)]^{1/2} C_{s+1,s}^r \\
 & - \frac{1}{(30)^{1/2}} R_{2,0} [r(r+1) - 3s^2] C_{ss}^r \\
 & - \frac{2s-1}{(20)^{1/2}} R_{2,1} [(r-s+1)(r+s)]^{1/2} C_{s-1,s}^r \\
 & + \frac{1}{(20)^{1/2}} \\
 & \cdot R_{2,2} [(r-s+1)(r+s)(r-s+2)(r+s-1)]^{1/2} C_{s-2,s}^r \\
 & - \sum_{l=0}^{\infty} \sum_{mm'=-l}^l \frac{l+r}{p=|l-r|} (-1)^r (i)^{p+r} \\
 & \cdot \left(\frac{2p+1}{2r+1} \right)^{1/2} C(lpr; m', s' - m') \\
 & \cdot C(lpr; m, s - m) \left[A_{mm'}^l + \frac{1}{kT} \frac{R_{00}}{(3)^{1/2}} l(l+1) B_{mm'}^l \right] \\
 & \cdot C_{s-m,s'-m'}^p \\
 & + \frac{1}{(2kT)^2} \frac{R_{00}}{(3)^{1/2}} \sum_{l=0}^{\infty} \sum_{mm'=-l}^l \sum_{u=0}^{\infty} \sum_{vv'=-u}^u B_{mm'}^l B_{vv'}^u \\
 & \cdot \sum_{g=|l-u|}^{l+u} \frac{1}{2} [g(g+1) - l(l+1) - u(u+1)] \\
 & \cdot C(lug; mv) C(lug; m'v') \sum_{p=|g-r|}^{g+r} \left(\frac{2p+1}{2r+1} \right)^{1/2} (i)^{r+p} \\
 & \cdot C(gpr; m+v, s-m-v) C(gpr; m'+v', s'-m'-v') \\
 & \cdot C_{s-m-v,s'-m'-v'}^p \\
 & + \frac{1}{(2kT)^2} (-1)^r \sum_{l=0}^{\infty} \sum_{mm'=-l}^l \sum_{u=0}^{\infty} \sum_{vv'=-u}^u B_{mm'}^l B_{vv'}^u \sum_{g=|l-u|}^{l+u} \\
 & \cdot \sum_{p=|g-r|}^{g+r} (i)^{p+r} \left(\frac{2p+1}{2r+1} \right)^{1/2} \\
 & \cdot C(lug; m'v') C(gpr; m'+v', s'-m'-v')
 \end{aligned}$$

$$\begin{aligned}
 & \cdot \left[-R_{2,-2} \frac{1}{(20)^{1/2}} [(l+m)(l-m+1)(u+v)(u-v+1)]^{1/2} \right. \\
 & \cdot C(lug; m-1, v-1) C(gpr; m+v-2, s-m-v+2) \\
 & \cdot C_{s-m-v+2,s'-m'-v'}^p \\
 & - R_{2,-1} \frac{1}{(20)^{1/2}} ([m[(u+v)(u-v+1)]^{1/2} C(lug; m, v-1) \\
 & + v[(l+m)(l-m+1)]^{1/2} C(lug; m-1, v)) \\
 & \cdot C(gpr; m+v-1, s-m-v+1) C_{s-m-v+1,s'-m'-v'}^p \\
 & + R_{2,0} \frac{1}{(120)^{1/2}} [g(g+1) - l(l+1) - u(u+1) - 6mv] \\
 & \cdot C(lug; mv) C(gpr; m+v, s-m-v) C_{s-m-v,s'-m'-v'}^p \\
 & + R_{2,1} \frac{1}{(20)^{1/2}} ([m[(u-v)(u+v+1)]^{1/2} C(lug; m, v+1) \\
 & + v[(l-m)(l+m+1)]^{1/2} C(lug; m+1, v)) \\
 & \cdot C(gpr; m+v+1, s-m-v-1) C_{s-m-v-1,s'-m'-v'}^p \\
 & - R_{2,2} \frac{1}{(20)^{1/2}} [(l-m)(l+m+1)(u-v)(u+v+1)]^{1/2} \\
 & \cdot C(lug; m+1, v+1) C(gpr; m+v+2, s-m-v-2) \\
 & \left. \cdot C_{s-m-v-2,s'-m'-v'}^p \right] = 0. \quad (A1)
 \end{aligned}$$

Rotational diffusion coefficients are expressed by spherical tensor as follows

$$R_{00} = D_p/3^{1/2} \quad (A2)$$

$$R_{2\pm 2} = -(D_{xx} - D_{yy} \pm 2iD_{xy})/2 \quad (A3)$$

$$R_{2\pm 1} = \pm(D_{xz} \pm iD_{yz}) \quad (A4)$$

$$R_{20} = (D_p - 3D_{zz})/6^{1/2}, \quad (A5)$$

where $D_p = D_{xx} + D_{yy} + D_{zz}$. $C(abc; d'b')$ is the Clebsch-Gordan coefficient (Rose, 1971).

The values of λ_n and expansion coefficients, $C_{s,s'}^r$, can be determined as eigen values and eigen vectors, respectively, by solving the kind of eigen value problem as in Eq. A1. The coefficients, $C_{s,s'}^r$, ($r = 0, 1, 2, \dots$; $s, s' = -r$ to r), are a set of eigen vectors corresponding to an eigen value, λ_m , ($\kappa = 1, 2, 3, \dots$). Constant coefficients of the simultaneous equations form a Hermite matrix. Therefore, eigen values of Eq. A1 should always be real.

We are indebted to Dr. and Mrs. Yamazaki of the Institute for Molecular Science for the measurements of fluorescence decay curves of apocytocrome *c*. We also thank Dr. T. Takano of Setsunan University for helpful discussions on the three-dimensional structure of cytochrome *c*. The authors thank the Computer Center, Institute for Molecular Science, Okazaki National Research Institutes for the use of the HITAC M-200 H.

Received for publication 13 May 1986 and in final form 26 September 1986

REFERENCES

Beechem, J. M., and L. Brand. 1985. Time-resolved fluorescence of proteins. *Annu. Rev. Biochem.* 54:43-71.

- Bernassau, J. M., E. D. Black, and D. M. Grant. 1982. Molecular motion in anisotropic medium. I. The effect of the dipolar interaction on nuclear spin relaxation. *J. Chem. Phys.* 76:253–256.
- Burghardt, T. P. 1983. Fluorescence depolarization by anisotropic rotational diffusion of a luminophore and its carrier molecule. *J. Chem. Phys.* 78:5913–5919.
- Burghardt, T. P. 1984. Model-independent fluorescence polarization for measuring order in a biological assembly. *Biopolymers.* 23:2383–2406.
- Burghardt, T. P. 1985. Time-resolved fluorescence polarization from ordered biological assemblies. *Biophys. J.* 48:623–631.
- Chuang, T. J., and K. B. Eisenthal. 1972. Theory of fluorescence depolarization by anisotropic rotational diffusion. *J. Chem. Phys.* 57:5094–5097.
- Dickerson, R. E., and R. Timkovich. 1975. Cytochrome *c*. In *The Enzymes*. Vol. 11. P. D. Boyer, editor. Academic Press, Inc., New York. 397–547.
- Favro, L. D. 1958. Rotational Brownian motion. In *Fluctuation Phenomena in Solids*. R. E. Burgess, editor. Academic Press Inc., New York. 79–101.
- Favro, L. D. 1960. Theory of rotational Brownian motion of a free rigid body. *Phys. Rev.* 119:53–62.
- Gurd, F. R. N., and T. M. Rothgeb. 1979. Motions in proteins. *Adv. Protein Chem.* 33:73–165.
- Hochstrasser, R. H., and D. K. Negus. 1984. Picosecond fluorescence decay of tryptophans in myoglobin. *Proc. Natl. Acad. Sci. USA.* 81:4399–4403.
- Jameson, D. M., and G. Weber. 1981. Resolution of the pH-dependent heterogeneous fluorescence decay of tryptophan by phase and modulation measurements. *J. Phys. Chem.* 85:953–958.
- Karplus, M., and J. A. McCammon. 1983. Dynamics of proteins: elements and function. *Annu. Rev. Biochem.* 52:263–300.
- Kinoshita, K., Jr., S. Kawato, and A. Ikegami. 1977. A theory of fluorescence polarization decay in membranes. *Biophys. J.* 20:289–305.
- Landau, L. D., and E. M. Lifshitz. 1983. *Quantum Mechanics: Non-relativistic Theory*. Translated to Japanese from the Russian. Tokyo Toshio, Inc., Tokyo. 795 pp.
- Nordio, P. L., G. Rigatti, and U. Serge. 1972. Spin relaxation in nematic solvents. *J. Chem. Phys.* 56:2117–2123.
- Polnaszek, C. F., G. V. Bruno, and J. H. Freed. 1973. ESR line shapes in the slow-motional region: anisotropic liquids. *J. Chem. Phys.* 58:3185–3199.
- Polnaszek, C. F., and J. H. Freed. 1975. Electron spin resonance studies of anisotropic ordering, spin relaxation, and slow tumbling in liquid crystalline solvents. *J. Chem. Phys.* 79:2283–2306.
- Rose, M. E. 1971. *Elementary Theory of Angular Momentum*. Translated to Japanese from the English. Misuzu Shobo, Tokyo. 246 pp.
- Sano, S., and K. Tanaka. 1964. Recombination of protoporphyrinogen with cytochrome *c* apoprotein. *J. Biol. Chem.* 239:PC3109–3110.
- Takano, T., and R. E. Dickerson. 1981. Conformation change of cytochrome *c*. I. Ferro cytochrome *c* structure refined at 1.5 Å resolution. *J. Mol. Biol.* 153:79–94.
- Tanaka, F., and N. Mataga. 1982. Dynamic depolarization of interacting fluorophores. Effect of internal rotation and energy transfer. *Biophys. J.* 39:129–140.
- Yamazaki, I., N. Tamai, H. Kume, H. Tsuchiya, and K. Oba. 1985. Microchannel-plate photomultiplier. Applicability to the time-correlated photon-counting method. *Rev. Sci. Instrum.* 56:1187–1194.